

# Localized eigenvectors on metric graphs

M. Brio<sup>\*1</sup>, J.-G. Caputo<sup>†2</sup> and H. Kravitz<sup>‡1</sup>

<sup>1</sup>Department of Mathematics, University of Arizona, Tucson, Arizona  
85721, USA.

<sup>2</sup>Laboratoire de Mathématiques, INSA de Rouen Normandie, 76801  
Saint-Etienne du Rouvray, France.

## Abstract

Motivated by the recent experimental work on random network fiber lasers [6, 7], we examine numerically the probability of observing localized eigenvectors in two arbitrary metric graphs. We find that exact localization is rare, and that it is necessary to tune the network to observe exactly localized states. We derive the resonance conditions to obtain localized eigenvectors for various geometric structures. Using the exact analytical form of the solution on each edge, we introduce a localization indicator based on the  $L_2$  norm. This indicator estimates the exact number of edges involved in a particular localized state and is more precise than the standard Inverse Participation Ratio (IPR).

## 1 Introduction

Partial differential equations (PDEs) on networks arise in many physical applications such as gas and water networks [1, 2], electromechanical waves in a

---

<sup>\*</sup>brio@math.arizona.edu

<sup>†</sup>caputo@insa-rouen.fr

<sup>‡</sup>hkravitz@math.arizona.edu

transmission grid [3], air traffic control [4], microwave networks [5] and random nanofiber lasers [6, 7] to name a few. In many cases, the problem can be linearized. Then separation of variables yields a Helmholtz (or Schrödinger) problem on the network. The associated eigenvalues and eigenvectors play a fundamental role in the theoretical analysis of the networks [8] and the practical applications.

The underlying mathematical model consists of a metric graph (a quantum graph in the Schrödinger context): a finite set of vertices connected by arcs (oriented edges) on which a metric is assigned. At the vertices, we can have different coupling conditions. The simplest assumes continuity of the field and zero total gradient at the vertices (Kirchhoff's law). The standard one-dimensional Laplacian together with these boundary conditions results in a generalized Laplacian and associated Helmholtz eigenvalue problem. It can be shown that with these coupling conditions (continuity and Kirchhoff's law) the operator is self-adjoint [8], yielding real eigenvalues and orthogonal eigenvectors. The eigenvectors form a complete basis of the appropriate set of square integrable functions on the graph. This spectral framework plays a key role in linear PDEs. We review and apply it in the present article.

Combinatorial or discrete graphs bear some similarities to metric graphs. In this type of graph, the edges only describe connections between vertices. For undirected graphs, both the adjacency matrix and the graph Laplacian are symmetric - they have real eigenvalues, and the eigenvectors can be chosen orthogonal. Eigenvectors can be localized on these graphs and this affects transport properties [9]. In a recent article [10] it was shown that the Laplacian eigenvectors of chains connected to complete graphs are highly localized in the complete graph regions where connectivity is high. These results were also found in the systematic study by Hata and Nakao [11] where they analyzed graphs with random degree distributions. The localization of eigenvectors found here is a purely topological effect because the Laplacian has equal weights. Random weights introduce additional complications. The pioneering 1958 study by Anderson [12] of a Schrödinger matrix equation with diagonal and off-diagonal random elements opened a very large field. For the past six decades, researchers have studied adjacency or Laplacian random matrices and described the properties of their eigenvectors. A recent example is the work by Slanina et al. [13] where an entropy indicator was introduced to measure localization. A more common indicator of localiza-

tion is the Inverse Participation Ratio (IPR), originally introduced by Bell and Dean [14]. Techniques from statistical mechanics yield insights on the properties of IPR for regular graphs; however it is difficult to give general results for arbitrary graphs.

In contrast to this large body of literature, localization of eigenvectors for random metric quantum graphs was only addressed in a handful of articles [15, 16, 17, 18]. Pankrashkin [17] showed that Anderson localization at all energies can be achieved by placing tan-like quasiperiodic  $\delta$ -interactions at the vertices of a quantum graph. For a 2D lattice with random lengths, Klopp and Pankrashkin [16] found Anderson localization at the minimum point of the spectrum. In [18], Hislop and Post proved that infinite radial tree-like random quantum graphs act as one-dimensional random Schrödinger operators exhibiting Anderson localization, e.g. almost surely pure point spectrum at all energies. To summarize, the situation is much more complex for metric graphs because topological effects combine with the randomness of the edge lengths.

Motivated by these results and experimental studies [6, 7], we asked the following question: in an arbitrary metric graph what is the probability of observing an exactly localized state? Such a state would correspond to the lasing from a network random laser [6]. To answer this question we undertook the numerical analysis of two graphs with random lengths using our systematic algorithm to compute arbitrary order eigenvalues and eigenvectors of any metric graph, see [19]. The eigenvectors have  $m$  components where  $m$  is the number of edges of the graph. The histogram of the  $L_2$  norms of the components revealed that exact localization is rare; one has to tune the network to observe a specific localized state. In a second part, we examined the conditions to observe exactly localized eigenvectors, starting from the simplest. We found the precise resonance conditions on the lengths and the eigenvalues for several geometric configurations such as a cycle, a triangle and a quadrilateral. We also ruled out single edge and degree three star configurations, thus showing that the most elementary localized eigenvector is a cycle and involves two edges. This prompted us to define a localization criterion adapted to these metric graphs based on the  $L_2$  norm. This quantity gives the number of edges involved in a localized eigenvector and is more precise than the IPR.

The article is organized as follows. The statement of the problem and a

brief review of the spectral properties of metric quantum graphs are provided in Section 2. In Section 3, we compute numerically the eigenvectors of two metric graphs. Section 4 lists exact resonant conditions for various geometric configurations. The localization criteria are discussed in Section 5. In Section 6, we discuss the results and conclude the article.

## 2 Spectrum of a metric graph

We recall the spectral theory formalism for completeness. Consider a finite metric graph with  $n$  vertices connected by  $m$  edges of length  $l_j$ ,  $j = 1 : m$ . Each edge is parameterized by its length and oriented arbitrarily from the origin vertex  $x = 0$  to the end vertex  $x = l_j$ . Following standard graph theory, we call these oriented edges arcs. We recall the definition of the *degree* of a vertex: it is the number of edges connected to it.

On this graph, we define the vector component wave equation

$$U_{tt} - \tilde{\Delta}U = 0, \quad (1)$$

where  $U \equiv (u_1, u_2, \dots, u_m)^T$ . Each component satisfies the one-dimensional wave equation inside the respective arc,

$$u_{jtt} - u_{jxx} = 0, \quad j = 1, 2, \dots, m \quad (2)$$

In addition, at the vertices the solution should be continuous and also satisfy the Kirchhoff flux conditions at each vertex of degree  $d$

$$\sum_{j=1}^d u_{jx} = 0, \quad (3)$$

where  $u_{jx}$  represent the outgoing fluxes for arc  $j$  emanating from the vertex.

Consider equation (1). Since the problem is linear, we can separate time and space and assume a harmonic solution  $U(x, t) = e^{ikt} V(x)$ . We then get a Helmholtz or Schrödinger eigenproblem for  $V$  on the graph

$$- \tilde{\Delta}V = k^2V, \quad (4)$$

together with the above-mentioned coupling conditions at the vertices and where  $\tilde{\Delta}$  is the generalized Laplacian, i.e. the standard Laplacian on the arcs together with the coupling conditions at the vertices. This generalized eigenvalue problem admits an inner product obtained from the standard inner product on  $L_2$  space - see [8]. We have

$$\langle f, g \rangle \equiv \sum_{\text{arc } j} \langle f_j, g_j \rangle, \quad \langle f_j, g_j \rangle = \int_0^{l_j} f_j(x)g_j(x)dx. \quad (5)$$

A solution in terms of Fourier harmonics on each branch  $j$  of length  $l_j$  is

$$v_j(x) = A_j \sin kx + B_j \cos kx. \quad (6)$$

It has been shown that, for the standard coupling conditions used here (continuity and Kirchhoff's condition), the eigenvectors  $V^i$  form a complete orthogonal basis of the Cartesian product  $L_2([0, l_1]) \times L_2([0, l_2]) \cdots \times L_2([0, l_m])$ , see [8]. Writing down the coupling conditions at each vertex, one obtains a homogeneous linear system whose  $k$ -dependent matrix is singular at the eigenvalues.

Using solution (6) on each arc with unknown coefficients  $A_j$  and  $B_j$ , the coupling conditions at each vertex yield the homogeneous system

$$M(k)X = 0, \quad (7)$$

of  $2m$  equations for the vector of  $2m$  unknown arc amplitudes

$$X = (A_1, B_1, A_2, B_2, \dots, A_m, B_m)^T.$$

The matrix  $M(k)$  is singular at the eigenvalues  $-k^2$ . We call these  $k$ -values resonant frequencies. A practical, robust computational algorithm for the computation of these eigenvalues and eigenvectors was proposed and studied in [19].

For each resonant frequency  $k_q$ , the eigenvectors  $V^q$  are determined from the null space of matrix  $M(k_q)$ . They can then be written as

$$V^q = \begin{pmatrix} A_1^q \sin k_q x + B_1^q \cos k_q x \\ A_2^q \sin k_q x + B_2^q \cos k_q x \\ \dots \\ A_m^q \sin k_q x + B_m^q \cos k_q x \end{pmatrix} \quad (8)$$

They can be normalized using the scalar product defined above. We have

$$\|V^q\|^2 = \langle V^q, V^q \rangle = \sum_{j=1}^m \langle V_j^q, V_j^q \rangle, \quad (9)$$

where  $V_j^q = A_j^q \sin k_q x + B_j^q \cos k_q x$  and  $\langle V_j^q, V_j^q \rangle$  is the standard scalar product on  $L_2([0, l_j])$ . This defines a broken  $L_2$  norm or graph norm. The scalar product  $\langle V_j^q, V_j^q \rangle$  can be computed explicitly

$$\langle V_j^q, V_j^q \rangle = \left( A_j^{q2} + B_j^{q2} \right) \frac{l_j}{2} + \frac{\sin 2k_q l_j}{4k_q} \left( -A_j^{q2} + B_j^{q2} \right) + A_j^q B_j^q \frac{1 - \cos 2k_q l_j}{2k_q}. \quad (10)$$

Once the eigenvalue problem is solved, one can proceed with the spectral solution of the time-dependent problem, exactly as for the one-dimensional wave equation on an interval. For that, expand the solution of the wave equation on the graph (1) using the eigenvectors,

$$U(x, t) = \sum_{q=1}^{\infty} a_q(t) V^q, \quad (11)$$

and obtain a simplified description of the dynamics in terms of the amplitudes  $a_q$ .

Note that we exclude all degree two vertices since due to continuity and Kirchhoff's condition, two edges sharing such a vertex can be merged into a single edge - see [20].

## 2.1 3-pumpkin graph

Let us consider the simple example of a two node graph connected by three edges of respective lengths  $l_1, l_2, l_3$  shown in Fig. 1. The term "pumpkin" was coined by Berkolaiko [20] who studied these graphs in detail. Following Berkolaiko's notation (see [21]), we use the term  $m$ -pumpkin, to emphasize the  $m$  edges between the two vertices.

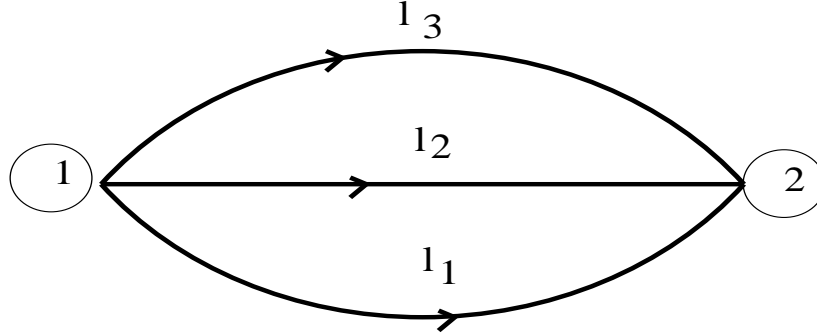


Figure 1: A two node graph with three edges.

To solve (4) on the 3-pumpkin described above, we write the solution in each branch  $j = 1, 2, 3$  as (6). At each node 1, 2, the solution is continuous and satisfies Kirchoff's law. We then get the following linear system

$$\begin{pmatrix} \cdot & 1 & \cdot & -1 & \cdot & \cdot \\ \cdot & 1 & \cdot & \cdot & \cdot & -1 \\ 1 & \cdot & 1 & \cdot & 1 & \cdot \\ s_1 & c_1 & -s_2 & -c_2 & \cdot & \cdot \\ s_1 & c_1 & \cdot & \cdot & -s_3 & -c_3 \\ c_1 & -s_1 & c_2 & -s_2 & c_3 & -s_3 \end{pmatrix} \begin{pmatrix} A_1 \\ B_1 \\ A_2 \\ B_2 \\ A_3 \\ B_3 \end{pmatrix} = \begin{pmatrix} 0 \\ 0 \\ 0 \\ 0 \\ 0 \\ 0 \end{pmatrix}, \quad (12)$$

where  $s_1 = \sin kl_1, c_1 = \cos kl_1, \dots$ . Setting the determinant of the matrix  $M(k)$  to 0, we obtain the equation for the eigenvalues  $k$ .

We choose the following parameters

$$l_1 = \sqrt{2}, \quad l_2 = \sqrt{3}, \quad l_3 = \sqrt{5}$$

The first three non zero eigenvalues  $k_i^2$  and corresponding eigenvectors  $V^i = (v_1^i, v_2^i, v_3^i)^T$  are given in Table 1 using the Fourier basis  $v_j^i(x) = A_j^i \sin k_i x + B_j^i \cos k_i x$

$i$	$k_i^2$	$A_1^i / B_1^i$	$A_2^i / B_2^i$	$A_3^i / B_3^i$
1	$(1.547901)^2 \approx 2.395998$	-0.24204	-0.53262	0.77466
		-0.12486	-0.12486	-0.12486
2	$(1.748474)^2 \approx 3.057162$	0.20191	0.03291	-0.23481
		-0.58105	-0.58105	-0.58105
3	$(2.016699)^2 \approx 4.067077$	0.85001	-0.69799	-0.15202
		0.123927	0.123927	0.123927

Table 1: First three non zero eigenvalues and eigenvectors for the 3-pumpkin graph with  $l_1 = \sqrt{2}$ ,  $l_2 = \sqrt{3}$ ,  $l_3 = \sqrt{5}$ .

## 2.2 Graph G14

We introduce the 14 edge graph - see Fig. 2. It was adapted from IEEE case 14, see [22], by eliminating the degree two vertices.

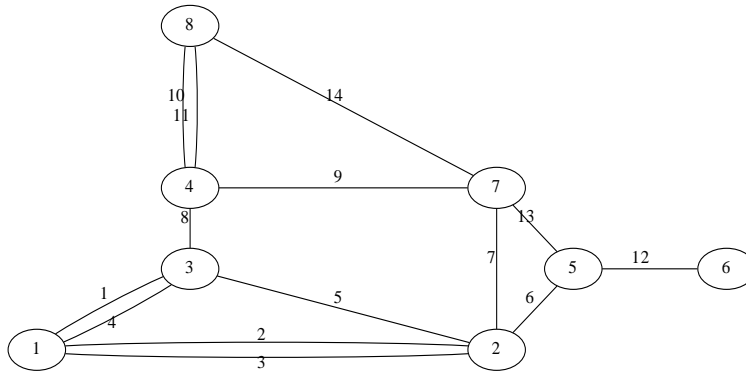


Figure 2: The 14 node graph

The lengths  $l_i, i = 1, \dots, m = 14$  are given in Table 2.

$l_1$ 11.91371443	$l_2$ 7.08276253	$l_3$ 6	$l_4$ 2.236067977	$l_5$ 4.123105626
$l_6$ 1.414213562	$l_7$ 2	$l_8$ 1	$l_9$ 4.7169892	$l_{10}$ 4.472135955
$l_{11}$ 2	$l_{12}$ 2	$l_{13}$ 1.414213562	$l_{14}$ 4.472135955	

Table 2: The lengths  $l_i$  for the graph G14 .

### 2.3 Buffon graph

We consider an example of a random graph, a Buffon's needle graph with 165 arcs and 104 vertices, see Fig. 3; to generate the graph we used a code developed by Michele Gaio, [6] for a random fiber laser application. To create the graph,  $n$  random points are uniformly generated on a square with diagonal  $L$ . A straight line segment (needle) with random angle and length is drawn from each point. The needles are all given the same diameter  $D$ . The intersections of line segments become the vertices of the graph. If two vertices are within a distance  $r = \left(\frac{12D}{L}\right)^2$  of each other, they are combined into a single vertex. The arcs of the graph are the lengths along the needles connecting the vertices. The resulting graph appears as a series of scattered needles. Most vertices have degree four and 15% of them have degree six.

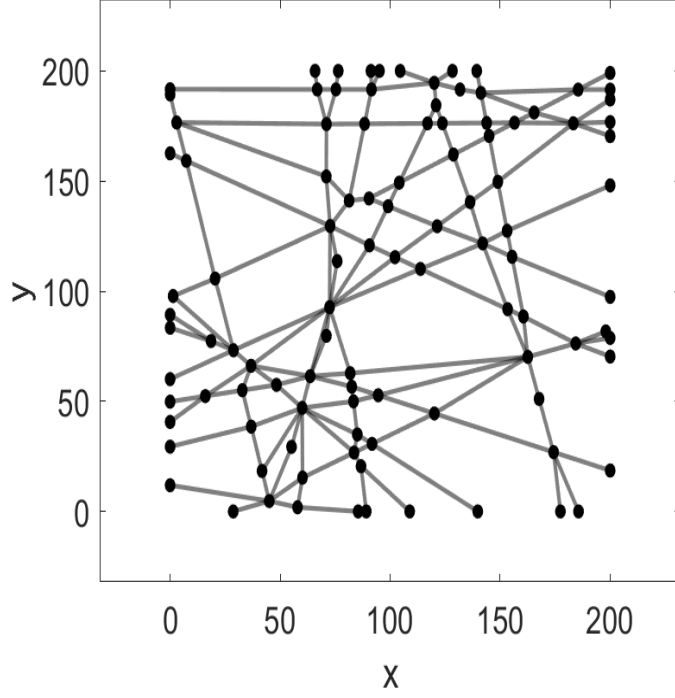


Figure 3: Buffon's needle graph.

### 3 Geometry of the eigenvectors: localization

To identify localized eigenvectors, we compute the  $L_2$  norm ratio

$$e_q(j) \equiv \frac{\langle V_j^q, V_j^q \rangle}{\langle V^q, V^q \rangle} \quad (13)$$

for each edge  $j = 1, 2, \dots, m$ .

### 3.1 Graph G14

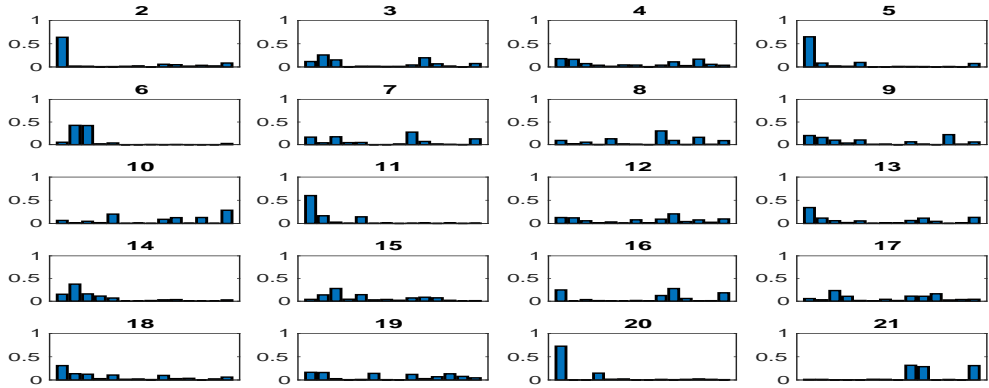


Figure 4: Histograms of the  $L_2$  norm ratio  $e_q(j)$  (13) for  $q = 2, \dots, 21$  from left to right and top to bottom for the G14 graph.

Fig. 4 presents the histograms of the  $L_2$  norm ratio  $e_q(j)$  for eigenvectors  $V^q$ ,  $q = 2, \dots, 21$  for the G14 graph. Note that  $q = 2, 5, 6, 11, 20$  and  $21$  correspond to eigenvectors where  $e_q(j) \geq 0.5$  for one or two edges  $j$  and  $e_q(j) < 0.05$  for the other edges. In Fig. 5 we present the localized eigenvectors corresponding to  $q = 2, 5, 6, 11, 20$  and  $21$ . For a given eigenvector  $V^q$ , we present for each edge  $j$  the quantity  $e_q(j)$  using the color code given in Table 3.

$e_q(j) < 0.06$	$0.06 < e_q(j) < 0.12$	$0.12 < e_q(j) < 0.2$	$0.2 < e_q(j)$
grey	pink	cyan	blue

Table 3: Color code for  $e_q(j)$ .

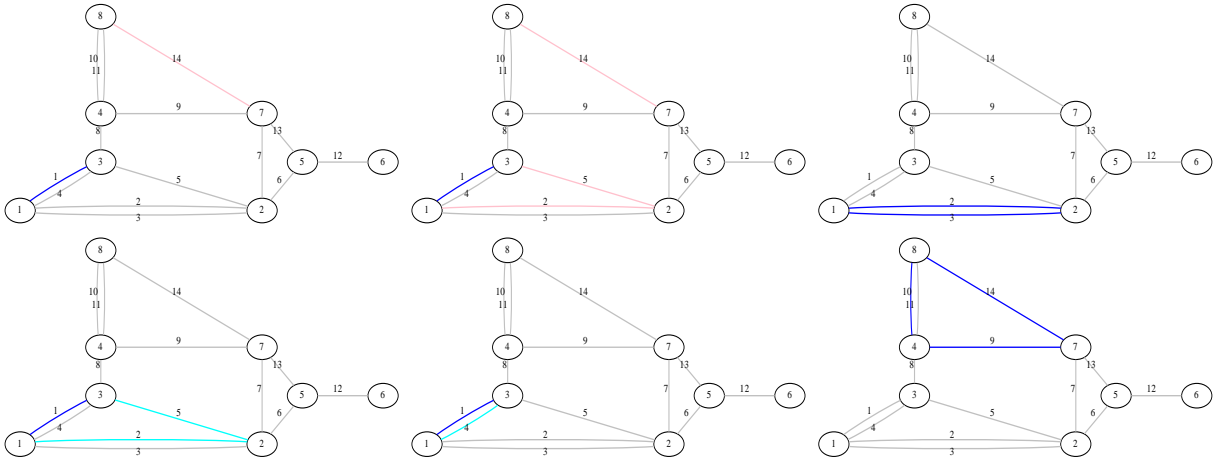


Figure 5: Localized eigenvectors  $V^q$  for  $q = 2, 5, 6, 11, 20$  and  $21$ . We present for each arc  $j$  the quantity  $e_q(j)$  with the color code given in Table 3. The values of  $k_q$  are given in the table below.

The values of  $k_q$  are presented in Table 4 below.

0.2347645148	0.4657835674	0.480197067
0.8078723081	1.3322287766	1.379308786

Table 4: The values of  $k_q$  shown in Fig. 5.

### 3.2 Buffon graph

Fig. 6 presents the histograms of the  $L_2$  norm ratio  $e_q(j)$  for eigenvectors  $V^q$ ,  $q = 2, \dots, 21$  for the Buffon graph.

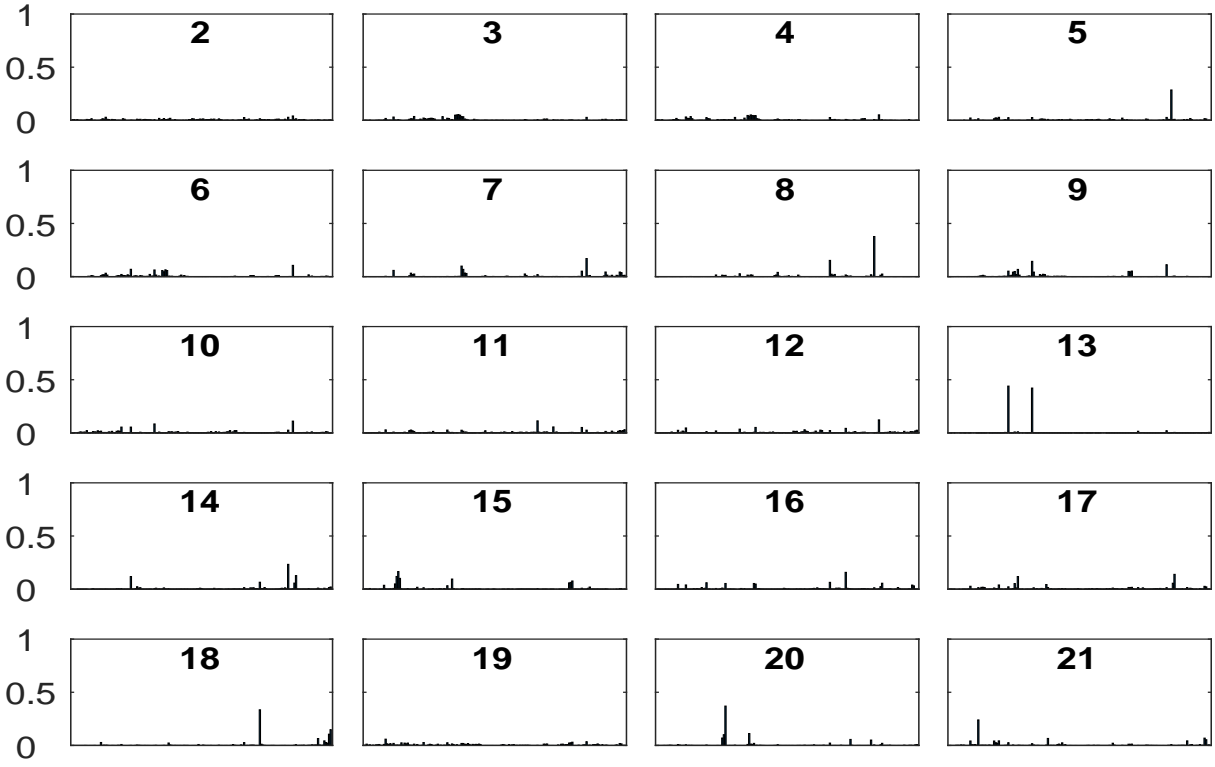


Figure 6: Histograms of the  $L_2$  norm ratio  $e_q(j)$  (13) for  $q = 2, \dots, 21$  from left to right and top to bottom for the Buffon graph.

The vectors  $V^q$  for  $q = 5, 8, 13, 18, 20$  and  $21$  are localized. They are plotted below.

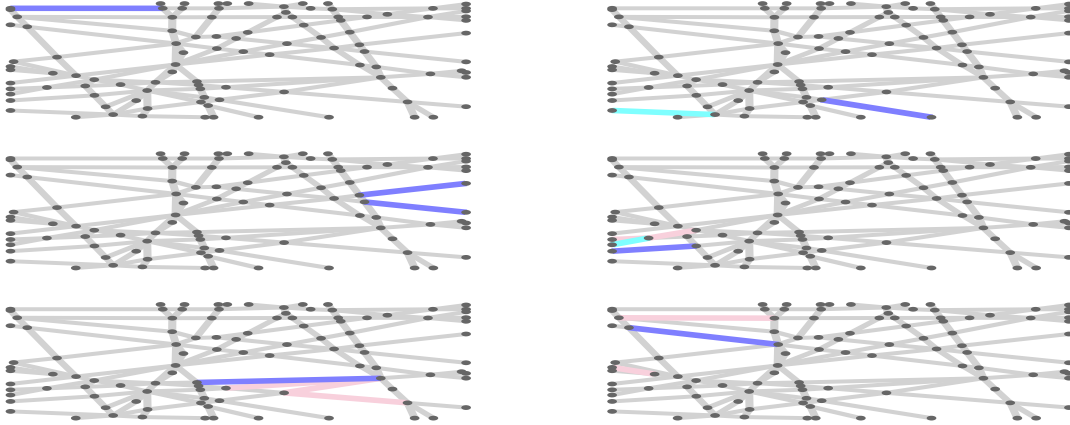


Figure 7: Plots of the localized eigenvectors  $V^q$  for  $q = 5, 8, 13, 18, 20$  and  $21$ . The color code is same as for Fig. 5.

The corresponding values of  $k_q$  are shown in Table 5

0.016866927	0.022719737	0.029337666
0.034764362	0.036236231	0.036802227

Table 5: The values of  $k_q$  shown in Fig. 7.

The results of this section show that for arbitrary metric graphs, localized eigenvectors do occur. However, this localization is not exact. For exactly localized eigenvectors to exist, we need a precise arrangement of the lengths of the arcs involved. In the next section, we give the conditions for exactly localized eigenvectors to exist.

## 4 Exact resonances

In the previous section, we observed that approximate localized states exist in graphs, especially for large  $k$ . Here we examine configurations that lead to *exact localized eigenvectors* where only a limited number of arcs have a nonzero component. We find that exactly localized eigenvectors can exist on

two connected leaves, as a 1-2 state in a pumpkin, as a triangle 1-2-3 and a quadrilateral 1-2-3-4. The analysis also enables us to rule out single arc, leaf, two connected arcs and degree three vertex resonances.

#### 4.1 Two connected leafs

Two connected leaves form the structure shown in Fig. 8.

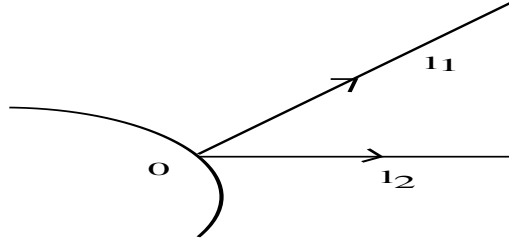


Figure 8: Two connected leaves in a graph.

To have an eigenvector exactly localized on the two leaves we need the following conditions on the two eigenvector components.

$$V_i = A_i \sin kx + B_i \cos kx, \quad i = 1, 2$$

$$\begin{aligned} V_1(0) &= V_2(0) = 0, \\ V_{1x}(0) + V_{2x}(0) &= 0, \\ V_{1x}(l_1) &= 0, \\ V_{2x}(l_2) &= 0, \end{aligned}$$

From this system of equations we get

$$\begin{aligned} A_1 + A_2 &= 0, \\ \cos kl_1 &= 0, \\ \cos kl_2 &= 0, \end{aligned}$$

so that

$$kl_1 = (2p + 1)\frac{\pi}{2}, \quad kl_2 = (2q + 1)\frac{\pi}{2}$$

These conditions are satisfied if  $l_1, l_2$  verify

$$(2p + 1)l_1 - (2q + 1)l_2 = 0$$

where  $p, q$  are integers.

Exactly localized eigenvectors also exist when there are three or more leaves. We sketch the situation for three leaves and give the result for more. Assume there are three leaves. The conditions are then

$$\begin{aligned} B_1 = B_2 = B_3 = 0, \quad A_1 + A_2 + A_3 = 0, \\ \cos kl_1 = \cos kl_2 = \cos kl_3 = 0. \end{aligned}$$

From this system we obtain the constraints on the lengths

$$\begin{aligned} (2p_1 + 1)l_1 - (2q_1 + 1)l_2 &= 0, \\ (2p_2 + 1)l_1 - (2q_2 + 1)l_3 &= 0, \\ (2p_3 + 1)l_2 - (2q_3 + 1)l_3 &= 0, \end{aligned}$$

where  $p_1, p_2, p_3, q_1, q_2, q_3$  are integers. Note that the eigenspace has dimension 2.

For  $l$  connected leaves, we would get an eigenspace of dimension  $l - 1$  and  $C_l^2$  constraints defining  $k$ .

## 4.2 1-2 and more resonances in a pumpkin subgraph

Consider the configuration of Fig. 9 where a pumpkin is embedded in a graph. Let us compute a solution that will be exactly localized in the 2-pumpkin with edge lengths  $l_1, l_2$ .

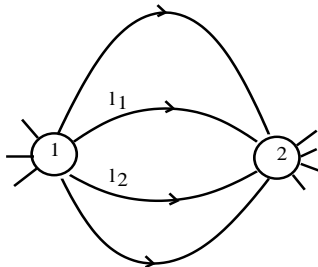


Figure 9: A 2-pumpkin 1-2 embedded in a graph.

For localization we want the following conditions

$$\begin{aligned} V_1(0) &= V_2(0) = 0, \\ V_1(l_1) &= V_2(l_2) = 0, \\ V_{1x}(0) + V_{2x}(0) &= 0, \\ V_{1x}(l_1) + V_{2x}(l_2) &= 0, \end{aligned}$$

This yields the system of equations

$$\begin{aligned} B_1 &= B_2 = 0, \\ A_1 \sin kl_1 &= A_2 \sin kl_2 = 0, \\ A_1 + A_2 &= 0, \\ A_1 \cos kl_1 + A_2 \cos kl_2 &= 0. \end{aligned}$$

We then obtain

$$\sin kl_1 = 0, \quad \sin kl_2 = 0,$$

so that

$$kl_1 = p\pi + 2q\pi, \quad kl_2 = r\pi + 2s\pi,$$

where  $p, q, r, s$  are integers. Then  $\cos kl_1 = (-1)^p$ ,  $\cos kl_2 = (-1)^r$ . A non-trivial solution  $A_1, A_2$  exists only if  $\cos kl_1 = \cos kl_2$  so that  $p$  and  $r$  have the same parity. The condition on the lengths is then

$$pl_2 - rl_1 = 0, \tag{14}$$

where  $p, r$  are integers of same parity.

To illustrate this exactly localized eigenvector, consider the graph shown in Fig. 10.

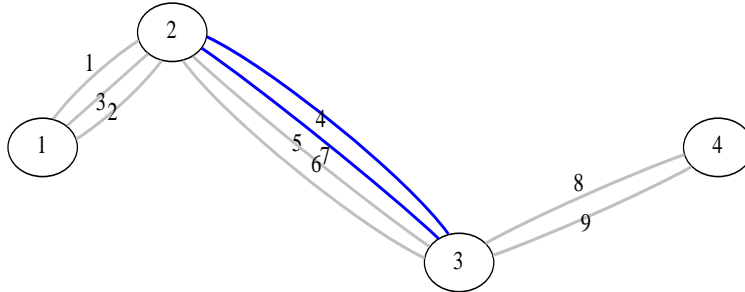


Figure 10: A graph showing an exactly localized 1-2 pumpkin eigenvector.

The lengths are given in Table 6, where the arcs 4 and 7 satisfy the resonance condition (14). The exactly localized eigenvector on arcs 4 and 7 is shown with the color code described in Table 3.

$l_1$ 2.236067977	$l_2$ 1.414213562	$l_3$ 1.732050807	$l_4$ $\pi$	$l_5$ $11 \pi$
$l_6$ 5.167771571	$l_7$ 9.424777960	$l_8$ 3.605551275	$l_9$ 5.693156148	

Table 6: The lengths  $l_i$  for the graph shown in Fig. 10.

Similarly, one can have an exactly localized eigenvector on a 3-pumpkin. The derivation is similar to the 2-pumpkin. We obtain the conditions

$$A_1 + A_2 + A_3 = 0,$$

$$\frac{l_1}{l_2} = \frac{p}{q}, \quad \frac{l_1}{l_3} = \frac{p}{r},$$

where  $p, q$  and  $r$  are integers of the same parity.

Note that the eigenspace has dimension 2.

### 4.3 Triangle 1-2-3

Consider the configuration of Fig. 11 where a triangle is embedded in a graph. Let us compute a solution that will be exactly localized in the triangle with edge lengths  $l_1, l_2, l_3$ .

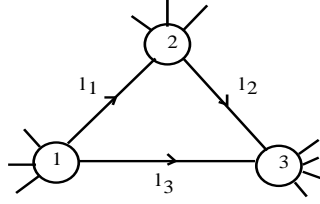


Figure 11: A triangle 1-2-3 embedded in a graph.

The conditions are

$$\begin{aligned}
 V_1(0) &= V_3(0) = 0, \\
 V_{1x}(0) + V_{3x}(0) &= 0, \\
 V_1(l_1) &= V_2(0) = 0, \\
 V_{1x}(l_1) - V_{2x}(0) &= 0, \\
 V_3(l_3) &= V_2(l_2) = 0, \\
 V_{3x}(l_3) + V_{2x}(l_2) &= 0,
 \end{aligned}$$

yielding

$$\begin{aligned}
 \frac{l_1}{l_2} &= \frac{n_1}{n_2}, \quad \frac{l_1}{l_3} = \frac{n_1}{n_3}, \\
 B_1 &= B_2 = B_3 = 0, \\
 A_3 &= -A_1, \\
 A_2 &= A_1 c_1, \\
 A_2 c_2 + A_3 c_3 &= 0,
 \end{aligned}$$

where  $n_1, n_2, n_3$  are integers and  $c_1 = \cos kl_1, \dots$ . Using the last relation, we get the condition

$$(-1)^{n_1+n_2} = (-1)^{n_3}, \quad (15)$$

so that  $n_1 + n_2 + n_3$  is even.

The eigenvector is

$$V = \sin kx(1, (-1)^{n_1}, -1)^T$$



The conditions are

$$\begin{aligned}
 V_0 &= V_A = V_B = V_C = 0, \\
 V_{1x}(0) - V_{4x}(l_4) &= 0, \\
 V_{1x}(l_1) - V_{2x}(0) &= 0, \\
 V_{2x}(l_2) - V_{3x}(0) &= 0, \\
 V_{3x}(l_3) - V_{4x}(0) &= 0,
 \end{aligned}$$

which imply

$$\begin{aligned}
 kl_i &= n_i\pi, \quad i = 1, \dots, 4 \\
 A_4c_4 - A_1 &= 0, \\
 A_1c_1 - A_2 &= 0, \\
 A_2c_2 - A_3 &= 0, \\
 A_3c_3 - A_4 &= 0,
 \end{aligned}$$

and  $n_1 + n_2 + n_3 + n_4$  even.

The eigenvector is

$$V = \sin kx((-1)^{n_4}, (-1)^{n_1+n_4}, (-1)^{n_1+n_2+n_4}, 1)^T$$

Fig. 14 shows such an exactly localized eigenvector on the quadrilateral 5-7-8-9 for the G14 graph where we chose

$$l_5 = 2\pi, \quad l_7 = 3\pi, \quad l_8 = 5\pi, \quad l_9 = 6\pi.$$

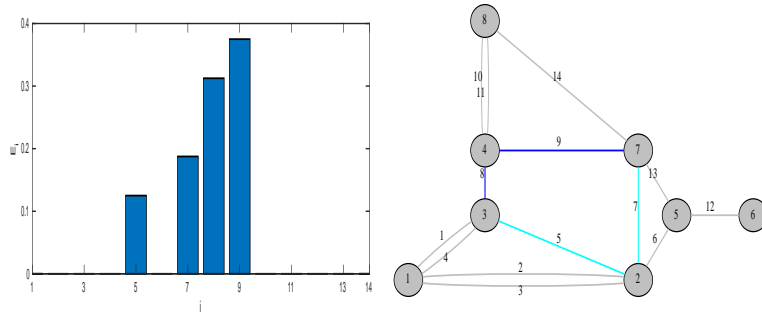


Figure 14: A quadrilateral 1-2-3-4 embedded in a graph. The active arcs are 5, 7, 8 and 9.

## 4.5 No single arc resonance

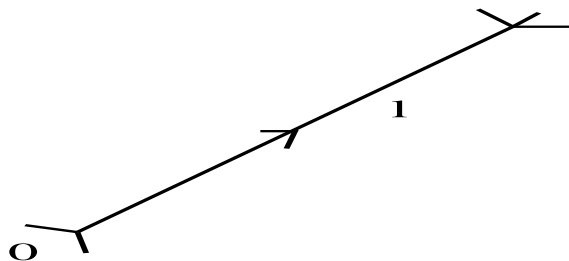


Figure 15: An arc embedded in a graph.

A localized state cannot exist on an arc embedded in a metric graph. To show this, consider Fig. 15. The localization conditions for the solution

$$V = A \sin kx + B \cos kx$$

are

$$V(0) = V(l) = 0, \quad V(0)_x = V_x(l) = 0$$

This yields  $A = B = 0$  so that a localized eigenvector cannot exist.

## 4.6 No leaf resonance

A leaf is an arc such that its end vertex has degree 1, see Fig. 16 for an illustration.

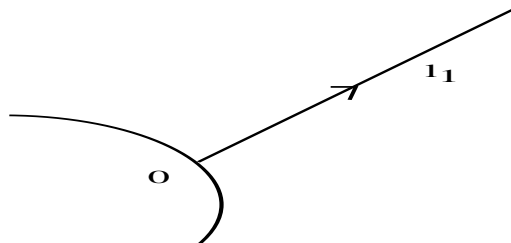


Figure 16: A leaf in a graph.

We will show that there are no exact resonances associated to such a structure of the graph.

Assume a leaf of length  $l$ , parameterized by  $x \in [0, l]$ . The boundary conditions at  $x = 0, l$  are  $V(0) = 0$ ,  $V_x(0) = V_x(l) = 0$ . Writing  $V$  as

$$V = A \sin kx + B \cos kx,$$

where all indices have been dropped for simplicity, we get from the first two conditions

$$A = B = 0,$$

so there are no eigenvectors localized on a leaf.

#### 4.7 No resonance on two connected arcs

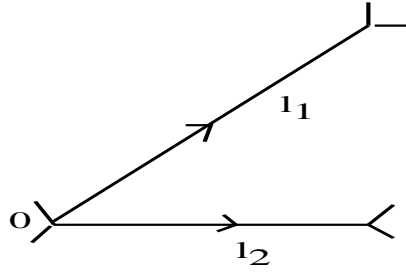


Figure 17: Two connected arcs "embedded" in a graph.

A localized state cannot exist on two arcs connected at one vertex. See Fig. 17 for an illustration. To show that such a state cannot exist, write out the localization conditions for the solution

$$\begin{aligned} V_1(0) &= V_2(0) = 0, \\ V_1(l_1) &= V_2(l_2) = 0, \\ V_{1x}(0) + V_{2x}(0) &= 0, \\ V_{1x}(l_1) + V_{2x}(l_2) &= 0, \end{aligned}$$

which yield the following system

$$\begin{aligned}
 B_1 &= B_2 = 0 \\
 A_1 s_1 &= 0 \\
 A_2 s_2 &= 0 \\
 A_1 c_1 + A_2 c_2 &= 0 \\
 A_1 c_1 &= 0 \\
 A_2 c_2 &= 0,
 \end{aligned}$$

which only has the solution  $A_1 = A_2 = 0$ , so a localized eigenvector cannot exist.

## 4.8 No degree three vertex resonance

Consider the configuration of Fig. 18 where a degree three vertex is embedded in a graph. No eigenvector can be localized on such a geometric structure. To see this let us compute a solution that will be exactly localized in the subgraph  $l_1, l_2, l_3$ .

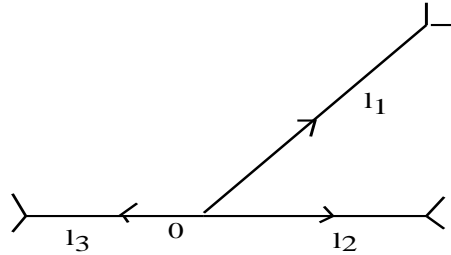


Figure 18: A degree three vertex "embedded" in a graph.

The conditions are

$$\begin{aligned}
 V_1(l_1) &= V_2(l_2) = V_3(l_3) = 0, \\
 V_{1x}(l_1) &= V_{2x}(l_2) = V_{3x}(l_3) = 0, \\
 V_{1x}(0) + V_{2x}(0) + V_{3x}(0) &= 0,
 \end{aligned}$$

yielding

$$\begin{aligned}
A_1 + A_2 + A_3 &= 0, \\
A_1 c_1 - B_1 s_1 &= 0, \\
A_2 c_2 - B_2 s_2 &= 0, \\
A_3 c_3 - B_3 s_3 &= 0, \\
A_1 s_1 + B_1 c_1 &= 0, \\
A_2 s_2 + B_2 c_2 &= 0, \\
A_3 s_3 + B_3 c_3 &= 0,
\end{aligned}$$

leading to the homogeneous linear system.

$$\begin{pmatrix}
1 & \cdot & 1 & \cdot & 1 & \cdot \\
c_1 & -s_1 & \cdot & \cdot & \cdot & \cdot \\
s_1 & c_1 & \cdot & \cdot & \cdot & \cdot \\
\cdot & \cdot & c_2 & -s_2 & \cdot & \cdot \\
\cdot & \cdot & s_2 & c_2 & \cdot & \cdot \\
\cdot & \cdot & \cdot & \cdot & c_3 & -s_3 \\
\cdot & \cdot & \cdot & \cdot & s_3 & c_3
\end{pmatrix}
\begin{pmatrix}
A_1 \\
B_1 \\
A_2 \\
B_2 \\
A_3 \\
B_3
\end{pmatrix}
=
\begin{pmatrix}
0 \\
0 \\
0 \\
0 \\
0 \\
0
\end{pmatrix}
\quad (16)$$

The determinant of the submatrix obtained by taking out the first line is equal to 1, so that the whole matrix has rank greater of equal to 6. Then there is no other solution than  $A_1 = B_1 = A_2 = B_2 = A_3 = B_3 = 0$ .

## 5 Localization criterion

The histograms of the energy components  $\langle V_j^q, V_j^q \rangle$  of the exactly localized eigenvectors show differences despite the fact that the  $A$  coefficients are the same. This imbalance is due to the different lengths of the arcs  $j$  because  $\langle V_j^q, V_j^q \rangle$  scales like  $l_j$ , see (10).

To correct the imbalance, we use equation (13) and rescale  $\langle V_j^q, V_j^q \rangle$  by  $l_j$ . For that we introduce the localization criterion for an eigenvector  $V^q$  as

$$\mathcal{L}_q = \max_j E_j^q, \quad (17)$$

where

$$E_j^q \equiv \frac{\langle V_j^q, V_j^q \rangle}{l_j \sum_k \frac{\langle V_k^q, V_k^q \rangle}{l_k}} \quad (18)$$

where we use the graph norm (9).

The calculations of the previous section for the two leaf, the triangle and the quadrilateral exact solutions can be used to exactly compute  $\mathcal{L}_q$ . The results are shown in Table 7.

	two leaf	triangle	quadrilateral
$\mathcal{L}_q$	1/2	1/3	1/4

Table 7: Localization criterion  $\mathcal{L}_q$  for three exactly localized eigenvectors.

To illustrate the usefulness of  $E_j^q$ , observe that the histograms presented in the left panels of Figs. 12 and 14 will have all the same amplitude if  $E_j^q$  is used instead of  $e_q(j)$  (13); the amplitudes will be 1/3 and 1/4 respectively. This shows that  $1/\mathcal{L}_q$  gives the number of active arcs. The analysis of the previous section shows that an eigenvector is localized on at least two arcs with equal amplitudes  $A_1 = A_2$ . Then a general upper bound is

$$\mathcal{L}_q \leq 0.5$$

The quantity  $E_j^q$  is the energy density of edge  $j$ . When applied to arbitrary metric graphs such as the G14, it indicates the regions of the graph that are most active.

In contrast, the standard localization criterion

$$IPR = \sum_{j=1}^m \frac{\int_0^{l_j} |V_j^q|^4 dx}{(\int_0^{l_j} |V_j^q|^2 dx)^2},$$

used for example by Gaio [6] does not give such precise information on the active arcs, as it is not based on exactly localized eigenvectors. The IPR does not provide information about the location of the localized mode, nor can it detect isolated modes that have neighboring edges with zero energy while the rest of the network is delocalized.

## 6 Discussion and conclusion

An important practical issue is how to excite these localized eigenvectors. For the random fiber laser, the authors of [6, 7] send an electromagnetic pulse

on a region of the network. They also couple the arcs on the boundary to an outside circuit to let energy escape. Then they expect that the only energy remaining will be the one corresponding to the exactly localized eigenvector.

This argument is correct in principle. To check it, consider the eigenvectors shown in Fig. 5. All localized modes are away from the vertex 6 so the components at that vertex are exponentially small. Assume a Sommerfeld radiation condition at that vertex,  $\epsilon U_t = U_x$ . Then the boundary condition there becomes

$$\epsilon V_{j_x} + ikV_j = 0,$$

which is easily satisfied if  $V_{j_x} = V_j = 0$ . This simple argument shows that exactly localized eigenvectors inside the graph will be preserved when the boundaries of the network are coupled to a dissipation source.

To summarize, we computed eigenvectors for two random metric graphs denoted as G14 and a Buffon graph and showed that exact localization is a rare event; to obtain it one needs to tune the network. We derived precise resonance conditions on the lengths and the eigenvalues for several geometric structures such as a cycle, a triangle and a quadrilateral. In addition, we showed that at least two edges are necessary for a localized state to exist. This prompted us to define a new localization criterion based on the  $L_2$  norm which gives the number of active edges, a quantity not available from the standard IPR criterion.

In the future, we plan to extend this study to non-Kirchhoff vertex conditions that correspond to various practical applications such as random network lasers. This would also require investigating the quality factor (energy decay rate) of these resonant structures under perturbations and leaky boundary conditions.

## References

- [1] Herty, M., Mohring, J., & Sachers, V. (2010). A new model for gas flow in pipe networks. *Mathematical Methods in the Applied Sciences*, 33(7), 845-855.

- [2] Martin, A., Klamroth, K., Lang, J., Leugering, G., Morsi, A., Oberlack, M., & Rosen, R. (Eds.). (2012). *Mathematical optimization of water networks* (Vol. 162). Springer Science & Business Media.
- [3] Kundur, P. *Power System Stability and Control*, 1. (1994) New York: McGraw-Hill
- [4] Work, D. B., & Bayen, A. M. (2008). Convex formulations of air traffic flow optimization problems. *Proceedings of the IEEE*, 96(12), 2096-2112.
- [5] Fu, Z., Koch, T., Antonsen, T. M., Ott, E., & Anlage, S. M. (2017). Experimental Study of Quantum Graphs with Simple Microwave Networks: Non-Universal Features. *Acta Physica Polonica, A.*, 132(6).
- [6] Gaio, M., Saxena, D., Bertolotti, J., Pisignano, D., Camposio, A., & Sapienza, R. (2019). A nanophotonic laser on a graph. *Nature communications*, 10(1), 1-7.
- [7] Cipolato, O., Mode controllability of a Network Random Laser, Master thesis, University of Padova, (2020).
- [8] Berkolaiko, G., & Kuchment, P. (2013). *Introduction to quantum graphs* (No. 186). American Mathematical Soc..
- [9] Caputo, J. G., Knippel, A., & Simo, E. (2012). Oscillations of networks: the role of soft nodes. *Journal of Physics A: Mathematical and Theoretical*, 46(3), 035101.
- [10] Caputo, J. G., Cruz-Pacheco, G., Knippel, A., & Panayotaros, P. (2020). Spectra of chains connected to complete graphs. *Linear Algebra and its Applications*, 605, 29-62.
- [11] Hata, S., & Nakao, H. (2017). Localization of Laplacian eigenvectors on random networks. *Scientific reports*, 7(1), 1-11.
- [12] Anderson, P. W. (1958). Absence of diffusion in certain random lattices. *Physical review*, 109(5), 1492.
- [13] Slanina, F. (2012). Localization of eigenvectors in random graphs. *The European Physical Journal B*, 85(11), 1-12.

- [14] Bell, R. J., & Dean, P. (1970). Atomic vibrations in vitreous silica. *Discussions of the Faraday society*, 50, 55-61.
- [15] Klopp, F., & Pankrashkin, K. (2008). Localization on quantum graphs with random vertex couplings. *Journal of Statistical Physics*, 131(4), 651-673.
- [16] F. Klopp, K. Pankrashkin: Localization on quantum graphs with random edge lengths. *Lett. Math. Phys.* 87 (2009) 99–114.
- [17] Klopp, F., & Pankrashkin, K. (2009). Localization on quantum graphs with random edge lengths. *Letters in Mathematical Physics*, 87(1), 99-114.
- [18] Hislop, P. D., & Post, O. (2009). Anderson localization for radial tree-like random quantum graphs. *Waves in Random and Complex Media*, 19(2), 216-261.
- [19] Brio, M., Caputo, J. G., & Kravitz, H. (2022). Spectral solutions of PDEs on networks. *Applied Numerical Mathematics*, 172, 99-117.
- [20] Berkolaiko, G. (2017). An elementary introduction to quantum graphs. *Geometric and computational spectral theory*, 700, 41-72.
- [21] Berkolaiko, G., Kennedy, J. B., Kurasov, P., & Mugnolo, D. (2017). Edge connectivity and the spectral gap of combinatorial and quantum graphs. *Journal of Physics A: Mathematical and Theoretical*, 50(36), 365201.
- [22] University of Illinois Information Trust Institute (2022), IEEE 14-Bus System, University of Illinois Board of Trustees, <https://icseg.iti.illinois.edu/ieee-14-bus-system/>.